XLVI CILAMCE
VITÓRIA - ES - BRAZIL - 2025
XLVI IBERO-LATIN AMERICAN CONGRESS ON COMPUTATIONAL METHODS IN ENGENEERING

# Nonlinear free axisymmetric vibration analysis of dielectric hyperelastic cylindrical shells

Alano R. Leal[1], Frederico M. A. Silva[1], Renata M. Soares[1]

[1]*School of Civil and Environmental Engineering, Federal University of Goiás*
*Av. Universitária, 1488, 74605-220, Goiás, Brazil*
*alanorodrigo@discente.ufg.br, silvafma@ufg.br, renatasoares@ufg.br*

**Abstract.** This work investigates the nonlinear free axisymmetric vibration of a cylindrical shell composed of an isotropic, homogeneous, incompressible, and dielectric hyperelastic material described by the Mooney-Rivlin constitutive model. The external static loading considers two cases: a uniform radial pressure and an axisymmetric radial pressure with the spatial distribution of the first axisymmetric vibration mode. Geometric nonlinearity is incorporated into the analytical model through Sanders-Koiter's nonlinear shell theory. The Rayleigh-Ritz method, combined with Hamilton's principle, is used to derive the set of nonlinear equilibrium equations. A comprehensive parametric study examines the effects of dielectric properties, and static preloading on the nonlinear frequency–amplitude relationship and static equilibrium paths. The results highlight significant changes in both static stability and nonlinear dynamic behavior, depending on the considered parameters and load conditions.

**Keywords:** Cylindrical shell, hyperelastic material, Dielectric, Geometric imperfections

## 1 Introduction

Soft active materials, particularly dielectric elastomers (DE), have garnered significant attention in various engineering fields due to their remarkable ability to undergo large deformations and convert electrical energy into mechanical work, and vice versa. This unique electromechanical coupling makes them highly promising for applications such as artificial muscles, soft robotics, sensors, and energy harvesting devices. Understanding their mechanical and electromechanical behaviors, especially under dynamic and nonlinear conditions, is crucial for the effective design and implementation of these innovative materials.

The study of shells, which are structural elements characterized by a curved average surface and a thickness significantly smaller than their other dimensions, is fundamental in engineering. These structures, which are also found in nature, have diverse applications, ranging from pressure vessels and aircraft fuselages to biological arteries and architectural domes. Their slender nature often makes them susceptible to high-amplitude vibrations and complex nonlinear phenomena, requiring advanced analytical and numerical models to accurately predict their behavior.

In the context of hyperelastic materials, which exhibit large and reversible deformations, the consideration of geometric and physical nonlinearities becomes necessary. Traditional linear elastic theories are insufficient to capture the intricate responses of these materials, especially when subjected to significant loads or undergoing large displacements. Prior research has extensively explored the nonlinear behavior of hyperelastic shells under various boundary conditions, material characteristics, and loading regimes. For instance, studies by Khaniki and Ghayesh [1] and Amabili [2] delve into the highly nonlinear statics and dynamics of such structures, highlighting complex phenomena in statics and dynamics analysis.

The integration of dielectric properties into hyperelastic materials introduces an additional layer of complexity due to the electromechanical coupling. Dielectric hyperelastic shells, when subjected to an electric field, deform due to Maxwell stresses, offering a pathway for electrically controlled actuation. This coupling can significantly alter the mechanical response, influencing static equilibrium paths, stability, and dynamic characteristics. Pioneering works by Goulbourne *et al.* [3–5] laid the groundwork for modeling these materials, focusing on nonlinear mathematical formulations for dielectric elastomer membranes and their dynamic responses. Specifically, the nonlinear oscillation of dielectric elastomer balloons and spherical shells has been a subject of interest, with researchers like Zhu *et al.* [6] investigating their dynamic behavior under combined pressure and voltage, and Zhao *et al.* [7] analyzing quasi-periodic and chaotic motions under alternating voltage. These studies reveal that

electric fields, alongside mechanical loads, can lead to complex nonlinear phenomena such as jumps in oscillation amplitude, bifurcations, and chaos, underscoring the need for detailed analyses.

This work contributes to the growing body of knowledge by investigating the nonlinear free axisymmetric vibration of cylindrical shells composed of an isotropic, homogeneous, incompressible, and dielectric hyperelastic material, described by the Mooney-Rivlin constitutive model. While previous research has explored various aspects of hyperelastic and dielectric structures, a comprehensive analysis of the nonlinear free axisymmetric vibration of dielectric hyperelastic cylindrical shells under diverse static preloading conditions, particularly with the spatial distribution of the first axisymmetric vibration mode, remains less explored. This work also provides insight into how dielectric properties and various static preloading configurations affect the nonlinear frequency-amplitude relationship and static equilibrium paths of these advanced structures. By incorporating geometric nonlinearity through Sanders-Koiter's nonlinear shell theory and employing the Rayleigh-Ritz method combined with Hamilton's principle, an analytical model is developed. The results are expected to enable advances in the study of both static stability and nonlinear dynamic behavior.

## 2 Mathematical formulation

A simply supported circular cylindrical shell, composed of an isotropic, homogeneous, incompressible and hyperelastic material of the Mooney-Rivlin type, is analyzed. This shell is subjected to a constant electric field distributed along the shell's thickness. The geometry of the shell with thickness $h$, radius $R$, length $L$ and density $\rho$, and the displacement field of the middle surface $u$, $v$ and $w$ as defined in the axial $x$, circumferential $\theta$ and lateral $z$ directions, in that respective order, are illustrated in Fig. 1. The boundary conditions are shown in eq. (1), where $u$, $v$ and $w$ are the axial, circumferential and transversal displacement fields, respectively, and, $M_x$ and $N_x$ are the internal axial bending moment and axial membrane force, respectively.

$$u_{,x} = v = w = M_x = N_x = 0 \qquad \text{at } x = 0, L. \tag{1}$$

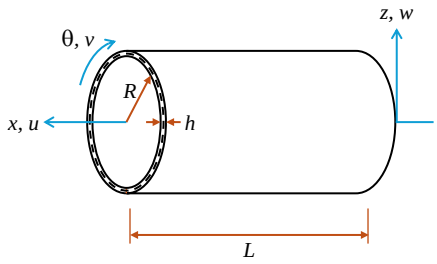



Figure 1. The cylindrical shell geometry, the coordinate system and the displacement fields.

The Euler-Lagrange equations, eq. (2), are used to derive the nonlinear equilibrium equations of the hyperelastic cylindrical shell, where $Lag = T - \Pi$ and $T$, eq. (3), is the kinetic energy, $\Pi$, eq. (4), is the internal potential deformation energy, and $N$ is the number of generalized coordinates $q_k$. In eq. (4), the second term inside the integrals is associated with the deformation energy induced by the constant electric field, $V$, applied across the shell's thickness. In this term, $\epsilon$ denotes the electric permittivity.

$$\frac{\mathrm{d}}{\mathrm{d}t}\left(\frac{\partial Lag}{\partial \dot{q}_k}\right) - \left(\frac{\partial Lag}{\partial q_k}\right) = Q_k, \qquad k = 1...N. \tag{2}$$

$$T = \frac{\rho h}{2}\int_0^L \int_0^{2\pi} \left(\dot{u}^2 + \dot{v}^2 + \dot{w}^2\right) R \,\mathrm{d}\theta \,\mathrm{d}x. \tag{3}$$

$$\Pi = \int_0^L \int_0^{2\pi} \int_{-\frac{h}{2}}^{\frac{h}{2}} \left( W + \frac{\epsilon V^2}{2\left(2\epsilon_{zz}+1\right)} \right) \mathrm{d}z \, R \, \mathrm{d}\theta \, \mathrm{d}x. \tag{4}$$

$$Q_k = -\frac{\partial R_e}{\partial \dot{q_k}} + \frac{\partial W_e}{\partial q_k}. \tag{5}$$

The generalized force $Q_k$, presented in eq. (2), is represented by both the non-conservative damping force, $R_e$, and the virtual work done by the external forces, $W_e$, as given by eq. (5). The non-conservative damping force $R_e$ is represented by a viscous damping force as shown in eq. (6), where $\beta_1$ is its damping coefficient. The virtual work done by the external forces $W_e$ is set in this study as a constant lateral pressure, defined in eq. (7), or as a harmonic axisymmetric load, given by eq. (8). In both cases, $p$ is the magnitude of the lateral pressure and the second term, given by a integral at the volume, represents the work done by electric field, where $\lambda_x$ and $\lambda_\theta$ are the stretch along the $x$ and $\theta$ directions, respectively.

$$R_e = \frac{1}{2} \beta_1 \, R \int_0^L \int_0^{2\pi} \dot{w}^2 \, \mathrm{d}\theta \, \mathrm{d}x, \qquad \beta_1 = 2 \, \eta_1 \, \rho \, h \omega_0. \tag{6}$$

$$W_e = \int_0^L \int_0^{2\pi} pwR \, \mathrm{d}\theta \, \mathrm{d}x + \frac{\epsilon V^2}{2h} \int_0^L \int_0^{2\pi} \int_{-\frac{h}{2}}^{\frac{h}{2}} \lambda_x \lambda_\theta^2 \, \mathrm{d}z \, R \, \mathrm{d}\theta \, \mathrm{d}x. \tag{7}$$

$$W_e = \int_0^L \int_0^{2\pi} p \sin\left(\frac{m\pi \, x}{L}\right) wR \, \mathrm{d}\theta \, \mathrm{d}x + \frac{\epsilon V^2}{2h} \int_0^L \int_0^{2\pi} \int_{-\frac{h}{2}}^{\frac{h}{2}} \lambda_x \lambda_\theta^2 \, \mathrm{d}z \, R \, \mathrm{d}\theta \, \mathrm{d}x. \tag{8}$$

This work investigates the nonlinear free vibration of the axisymmetric modes of the hyperelastic shell. So, it is useful to present the modal solutions used to describe the transversal displacement field $w(x,t)$, eq. (9), and the axial displacement field $u(x,t)$, eq. (10). These modal displacement field satisfy the boundary conditions of eq. (1).

$$w(x,t) = \sum_{j=1}^{J} w_{j0}\,(t) \sin\left(\frac{(2j-1)\, m\pi \, x}{L}\right) \tag{9}$$

$$u(x,t) = \sum_{j=1}^{J} u_{j0}\,(t) \cos\left(\frac{(2j-1)\, m\pi \, x}{L}\right) \tag{10}$$

where $m$ is the axial half-wave number of the axisymmetric natural vibration mode; and, $w_{j0}(t)$ and $u_{j0}(t)$ are the axisymmetric modal amplitudes in the transversal and axial directions, respectively. The vector of generalized coordinates is expressed in terms of these modal amplitudes as $q_k = [w_{j0}(t), u_{j0}(t)]$.

Returning to eq. (4), the energy density function, $W$, incorporates the nonlinear stress-strain relationship into the system and, in this work, is defined by the Mooney-Rivlin hyperelastic constitutive model, as follows:

$$W = \mu_1 \left(I_1 - 3\right) + \mu_2 \left(I_2 - 3\right), \tag{11}$$

where $\mu_1$ and $\mu_1$ are material parameters; and $I_1$ and $I_2$ are the first and second deformation invariants, respectively.

To describe these deformation invariants, the right Cauchy-Green deformation tensor $\mathbf{C}$ is used, and it can be obtained from the Green-Lagrange deformation tensor $\mathbf{E}$ and the identity matrix $\mathbf{I}$, according to eq. (12). Therefore, the expressions for the deformation invariants are defined according to eq. (13). The Jacobian $\mathbf{J}$, relative to the third invariant and necessary to assure the incompressibility hypothesis, is a also assumed. According to the right Cauchy-Green deformation tensor $\mathbf{C}$, the stretches along the $x$, $\theta$, and $z$ directions are expressed in eq. (14).

$$\mathbf{C} = 2\mathbf{E} + \mathbf{I} = \begin{bmatrix} 2\,\epsilon_{xx} + 1 & \gamma_{x\theta} & 0 \\ \gamma_{x\theta} & 2\,\epsilon_{\theta\theta} + 1 & 0 \\ 0 & 0 & 2\,\epsilon_{zz} + 1 \end{bmatrix}. \tag{12}$$

$$\begin{aligned} I_1 =& \mathrm{tr}\,(\mathbf{C}) = 2\,(\epsilon_{xx} + \epsilon_{\theta\theta} + \epsilon_{zz}) + 3. \\ I_2 =& \frac{1}{2}\left\{[\mathrm{tr}\,(\mathbf{C})]^2 - \mathrm{tr}\left(\mathbf{C}^2\right)\right\} = 4\,(\epsilon_{xx} + \epsilon_{\theta\theta} + \epsilon_{zz} + \epsilon_{xx}\epsilon_{\theta\theta} + \epsilon_{xx}\epsilon_{zz} + \epsilon_{\theta\theta}\epsilon_{zz}) - \gamma_{x\theta}^2 + 3. \\ I_3 =& J^2 = \det\,(\mathbf{C}) = (2\,\epsilon_{zz} + 1)\left((2\,\epsilon_{xx} + 1)\,(2\,\epsilon_{\theta\theta} + 1) - {\gamma_{x\theta}}^2\right). \end{aligned} \tag{13}$$

$$\lambda_x = \sqrt{2\epsilon_{xx} + 1} \quad \lambda_\theta = \sqrt{2\epsilon_{\theta\theta} + 1} \quad \lambda_z = \sqrt{2\epsilon_{zz} + 1}. \tag{14}$$

where $\epsilon_{xx}$, $\epsilon_{\theta\theta}$ and $\gamma_{x\theta}$ are the components of the Green-Lagrange deformation tensor $\mathbf{E}$, and they are given by the nonlinear Sanders-Koiter theory, as presented in eq. (15). It is important to note that, since this work investigates only axisymmetric vibration, the deformation field eq. (16), and the change in curvature, eq. (17), of the middle surface of the hyperelastic shell are significantly simplified by neglecting both the circumferential dependence of the displacement fields and the differential terms related to the circumferential coordinate.

$$\epsilon_{xx} = \epsilon_{x,0} + zk_x, \epsilon_{\theta\theta} = \epsilon_{\theta,0} + zk_\theta, \gamma_{x\theta} = \gamma_{x\theta,0} + zk_{x\theta} \tag{15}$$

where

$$\epsilon_{x,0} = \frac{\partial u}{\partial x} + \frac{1}{2}\left(\frac{\partial w}{\partial x}\right)^2, \epsilon_{\theta,0} = \frac{w}{R}, \gamma_{x\theta,0} = 0 \tag{16}$$

$$k_x = -\frac{\partial^2 w}{\partial x^2}, k_\theta = 0, k_{x\theta} = 0 \tag{17}$$

To represent the transverse normal strain $\epsilon_{zz}$, the condition of Jacobian be equal to one is applied to consider the hyperelastic material as incompressible. So, with the appropriate algebra, the following equation is obtained:

$$\epsilon_{zz} = \frac{1}{2\,((2\,\epsilon_{xx} + 1)\,(2\,\epsilon_{\theta\theta} + 1) - {\gamma_{x\theta}}^2)} - \frac{1}{2}. \tag{18}$$

In this work, eq. (19) is expanded in terms of $\epsilon_{xx}$, $\epsilon_{\theta\theta}$ and $\gamma_{x\theta}$ up to the fourth order, obtaining the approximated expression for $\epsilon_{zz}$ as:

$$\begin{aligned} \epsilon_{zz} \approx& -(\epsilon_{xx} + \epsilon_{\theta\theta}) + 2\left(\epsilon_{xx}^2 + \epsilon_{\theta\theta}^2 + \epsilon_{xx}\epsilon_{\theta\theta}\right) - 4\left(\epsilon_{xx}^3 + \epsilon_{\theta\theta}^3 + \epsilon_{xx}^2\epsilon_{\theta\theta} + \epsilon_{xx}\epsilon_{\theta\theta}^2\right) \\ &+ 8\left(\epsilon_{xx}^4 + \epsilon_{\theta\theta}^4 + \epsilon_{xx}^3\epsilon_{\theta\theta} + \epsilon_{xx}\epsilon_{\theta\theta}^3 + \epsilon_{xx}^2\epsilon_{\theta\theta}^2\right) \end{aligned} \tag{19}$$

The next numerical results are presented using the following non-dimensional parameters:

$$P = \frac{p}{\mu_1}, \quad \lambda^2 = \frac{\epsilon V^2}{\mu_1}, \quad \alpha = \frac{\mu_2}{\mu_1}. \tag{20}$$

## 3 Numerical results

Consider a perfect hyperelastic cylindrical shell subjected to a constant electric field applied along the thickness. The geometric and physical parameters are defined as: radius $R = 0.1\,m$, length $L = 0.1538\,m$, thickness $h = 0.0005\,m$, density $\rho = 1100\,kg/m^3$, and material properties $\mu_1 = 416185.5\,Pa$ and $\mu_2 = -498.8\,Pa$ ($\alpha = -0.0012$). In this work, only the nonlinear axisymmetric deformation and free vibration are analyzed, with particular attention to the influence of the electric field, $\lambda$, on these responses.

Initially, the influence of the electric field on the nonlinear static displacement is investigated. Both lateral axisymmetric pressure distributions, constant and shaped according to the first mode, defined by eqs. (7) and (8), respectively, are considered in this analysis. To this end, the modal solutions of eqs. (9) and (10), previously validated for convergence up to displacements 50 times the shell thickness with $J = 3$, are employed to derive the discretized system of equilibrium equations.

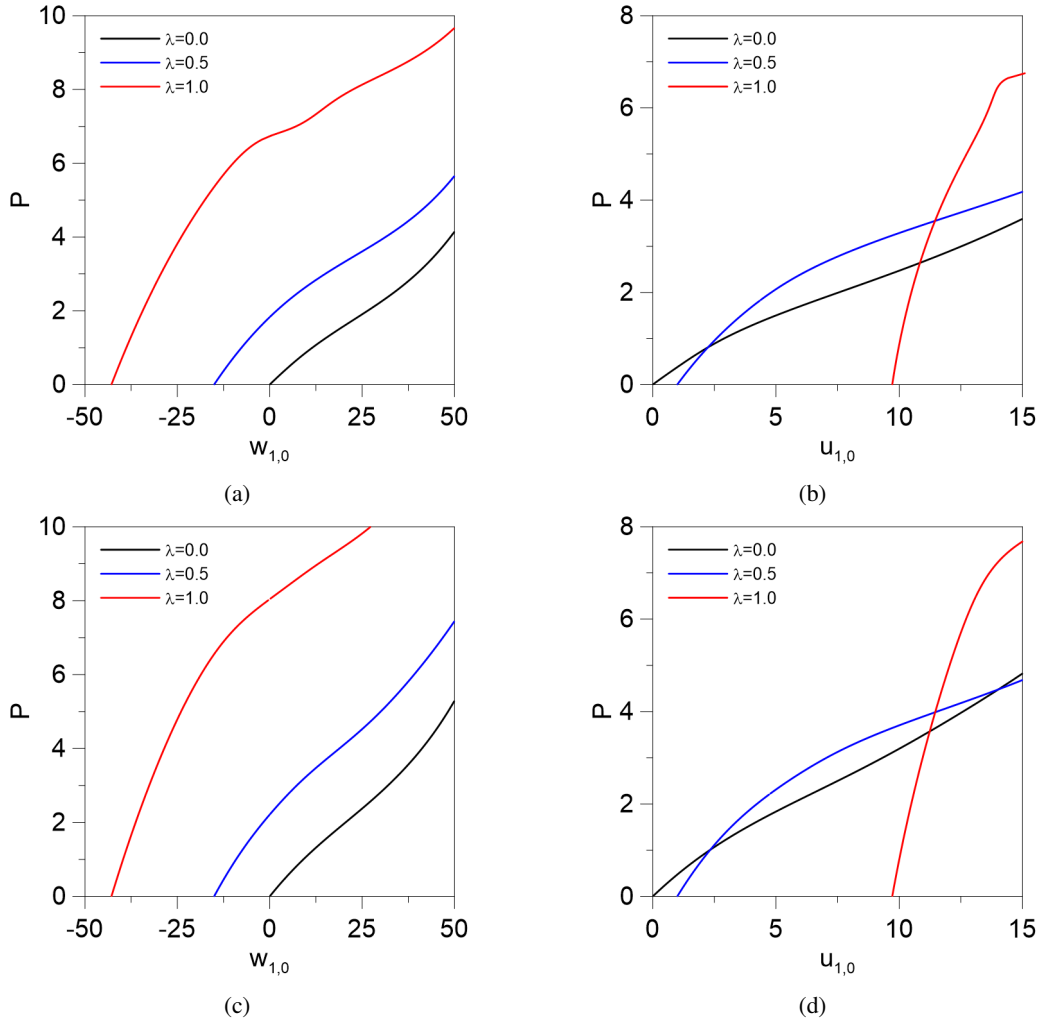
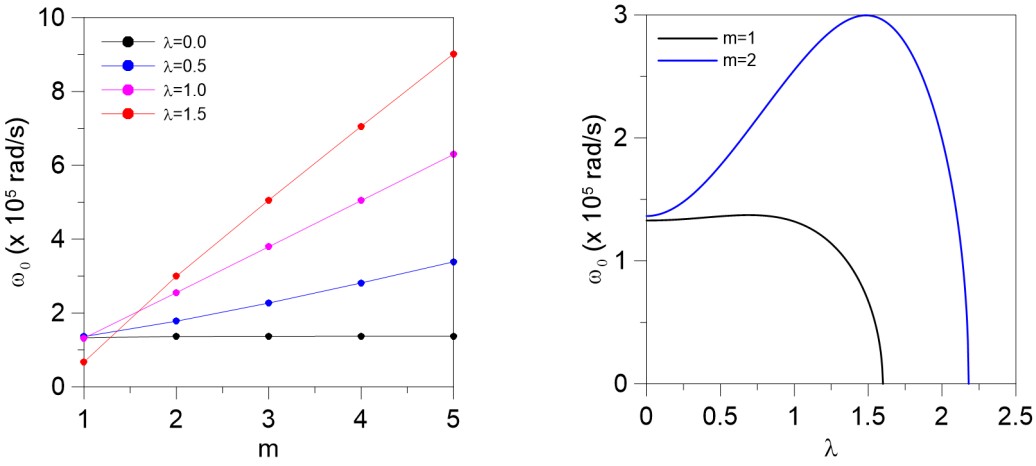



Figure 2. Nonlinear static equilibrium paths considering (a, b) a constant pressure and (c, d) a pressure in the shape of first transversal mode for different values of electric field. (a, c) first transversal modal amplitude $w_{1,0}$ and (b, d) first axial modal amplitude $u_{1,0}$.

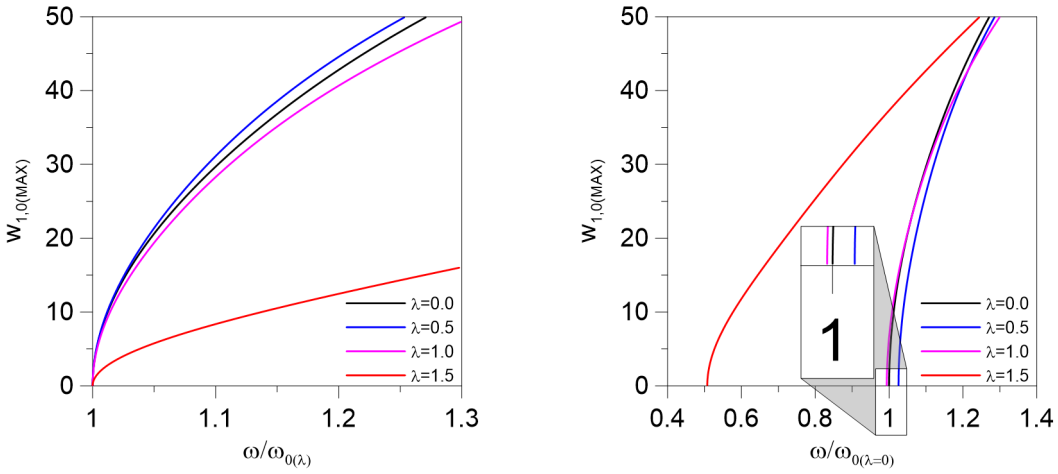
Figure 2 shows the variation of the first modal amplitudes of the transversal and axial displacement fields as a function of the applied lateral pressure magnitude, for different values of the electric field. From this figure, it can be observed that the hyperelastic cylindrical shell exhibits a nonlinear equilibrium path, where the modal

amplitudes increase with the magnitude of the lateral pressure. The transversal modal amplitude, $w_{1,0}$, assumes values greater than the axial modal amplitude, $u_{1,0}$, regardless of the applied lateral pressure distribution. The electric field induces an initial displacement when applied. As considered in the deformation energy and the work done by the electric field, the parameter $\lambda$ reduces the transversal modal amplitude $w_{1,0}$ as its value increases. Conversely, the axial modal amplitude $u_{1,0}$ increases with the growth of the electric field parameter $\lambda$.




(a) (b)

Figure 3. (a) Axisymmetric frequency spectrum of the hyperelastic cylindrical shell for different values of the electric field. (b) Variation of the natural frequencies of the first two modes with the applied electric field. ($P = 0$)




(a) (b)

Figure 4. Nonlinear frequency-amplitude relation (backbone curve) normalized in respect to (a) the natural frequency of each case of $\lambda$ (b) the natural frequency of the case without electric field, $\lambda = 0$. ($m = 1$, $P = 0$).

Now, considering a free dynamic analysis, the natural frequencies of the hyperelastic shell are presented for different axisymmetric modes and electric field values. These frequencies are obtained from the linearized discretized equations, which lead to a classical eigenvalue/eigenvector problem. To this end, the modal amplitudes are discretized in time as $w_{i,0}(t) = \overline{w}_{i,0}\cos(\omega t)$ and $u_{i,0}(t) = \overline{u}_{i,0}\cos(\omega t)$. As presented in Fig. 3a, the natural frequencies increase as the half-wave number increases. The electric field increases the natural frequencies for $m \geq 2$ as $\lambda$ increases, at least for the cases of $\lambda$ analyzed. On the other hand, for $m = 1$, the natural frequencies are $13284.6\,rad/s$, $13624.0\,rad/s$, and $13201.0\,rad/s$ for $\lambda = 0$, $0.5$, and $1.0$, respectively. These results indicate that the electric field does not produce a unique effect on the natural frequencies, i.e, the frequency does not always increase with the parameter $\lambda$. The frequency may either increase or decrease as $\lambda$ increases, depending on the specific mode being analyzed. This suggests that the electric field can render a vibration mode unstable, leading to an imaginary frequency value. To investigate this aspect, Fig. 3b presents the variation of the natural frequencies of the first two axisymmetric modes with the parameter $\lambda$. As shown in this figure, there is a value of $\lambda$ at which the natural frequency of the investigated mode vanishes, indicating the onset of instability.

The influence of the electric field on the nonlinear frequency–amplitude relationship (backbone curve) is also evaluated. For this purpose, the nonlinear discretized equations, discretized in time, are considered. Fig. 4 displays the backbone curves of the hyperelastic shell for different values of the electric field parameter, $\lambda$. In Fig. 4a, the nonlinear frequencies, $\omega$, are normalized with respect to the linear frequency of the hyperelastic shell for each evaluated value of $\lambda$. Conversely, in Fig. 4b, the nonlinear frequencies are normalized relative to the linear frequency of the shell without an electric field ($\lambda = 0$). As observed in Fig. 4a, the backbone curves exhibit nonlinear dynamic behavior influenced by the electric field. Notably, for $\lambda = 0.5$, the backbone displays a reduced hardening effect compared to the case without an electric field ($\lambda = 0.0$). For higher values of $\lambda$, the hardening effect of the backbone curves increases. In Fig. 4b, it is noted that the backbone curves shift either to the left or to the right of the backbone curve corresponding to the shell with $\lambda = 0$, depending on whether the natural frequency of the hyperelastic shell with $\lambda \neq 0$ decreases or increases, respectively.

## 4 Conclusions

In this work, a dynamic model was developed for simply supported circular cylindrical shells composed of isotropic, homogeneous, incompressible, and hyperelastic material to investigate nonlinear axisymmetric displacements and free vibration. A constant electric field applied along the shell's thickness was also considered. Both geometric and material nonlinearities were accounted for by employing the Sanders-Koiter nonlinear shell theory and the Mooney-Rivlin hyperelastic constitutive law. The system of dynamic equations was derived using the Rayleigh-Ritz method combined with the Euler-Lagrange equations. The modal displacement field considered includes only axisymmetric modes. Initially, two types of axisymmetric transversal pressure loadings, constant and shaped according to the first mode, were applied to obtain the nonlinear equilibrium curves and to analyze the influence of the electric field on these responses. In the dynamic analysis, the effect of the electric field was also investigated by evaluating its influence on the natural frequencies and the nonlinear frequency–amplitude relationship. In both nonlinear static and dynamic analyses, the presence of the electric field significantly altered the nonlinear behavior of the hyperelastic shell, modifying the hardening effects observed in the frequency–amplitude relation and the equilibrium curves. Another important aspect highlighted is the stability of the vibration modes, which depends on the magnitude of the electric field.

**Acknowledgements.** The authors are grateful for the financial support provided by CAPES, CNPq and FAPEG for the development of this work.

**Authorship statement.** The authors hereby confirm that they are the sole liable persons responsible for the authorship of this work, and that all material that has been herein included as part of the present paper is either the property (and authorship) of the authors, or has the permission of the owners to be included here.

## References

[1] H. B. Khaniki and M. H. Ghayesh. A general nonlinear formulation for the static and dynamic analysis of hyperelastic shells. *International Journal of Non-Linear Mechanics*, vol. 145, pp. 104188, 2023.
[2] M. Amabili. *Nonlinear Mechanics of Shells and Plates in Composite, Soft and Biological Materials*. Cambridge University Press, Cambridge, 2018.
[3] N. C. Goulbourne, E. M. Mockensturm, and M. I. Frecker. A nonlinear model for dielectric elastomer membranes. *Journal of Applied Mechanics*, vol. 72, n. 5, pp. 651–657, 2005.
[4] E. M. Mockensturm and N. Goulbourne. Dynamic response of dielectric elastomers. *International Journal of Non-Linear Mechanics*, vol. 41, n. 3, pp. 388–395, 2006.
[5] N. C. Goulbourne, E. M. Mockensturm, and M. I. Frecker. Electro-elastomers: Large deformation analysis of silicone membranes. *International Journal of Solids and Structures*, vol. 44, n. 8, pp. 2609–2626, 2007.
[6] J. Zhu, S. Cai, and Z. Suo. Nonlinear oscillation of a dielectric elastomer balloon. *Polymer International*, vol. 59, n. 3, pp. 305–312, 2010.
[7] Y. Tang, Z. Zhao, X. Yuan, R. Wang, and Z. Wang. Periodic and chaotic vibrations of dielectric elastomer spherical shells considering structural damping. *Nonlinear Dynamics*, pp. 1–16, 2024.